Quenching and partitioning martensite—A novel steel heat treatment

D.V. Edmonds [a,*], K. He [a], F.C. Rizzo [b], B.C. De Cooman [c], D.K. Matlock [d], J.G. Speer [d]

[a] *Institute for Materials Research, University of Leeds, Leeds LS2 9JT, United Kingdom*
[b] *Department of Materials Science and Metallurgy, Pontificia Universidade Catolica-Rio de Janeiro, RJ 22453-900, Brazil*
[c] *Department of Metallurgy and Materials Science, Ghent University, BE-9052 Ghent, Belgium*
[d] *Advanced Steel Processing and Products Research Centre, Colorado School of Mines, Golden, CO 80401, USA*

Abstract

A novel concept for the heat treatment of martensite, different to customary quenching and tempering, is described. This involves quenching to below the martensite-start temperature and directly ageing, either at, or above, the initial quench temperature. If competing reactions, principally carbide precipitation, are suppressed by appropriate alloying, the carbon partitions from the supersaturated martensite phase to the untransformed austenite phase, thereby increasing the stability of the residual austenite upon subsequent cooling to room temperature. This novel treatment has been termed 'quenching and partitioning' (Q&P), to distinguish it from quenching and tempering, and can be used to generate microstructures with martensite/austenite combinations giving attractive properties. Another approach that has been used to produce austenite-containing microstructures is by alloying to suppress carbide precipitation during the formation of bainitic structures, and interesting comparisons can be made between the two approaches. Moreover, formation of carbide-free bainite during the Q&P partitioning treatment may be a reaction competing for carbon, although this could also be used constructively as an additional stage of Q&P partitioning to form part of the final microstructure. Amongst the ferrous alloys examined so far are medium carbon bar steels and low carbon formable TRIP-assisted sheet steels.
© 2006 Elsevier B.V. All rights reserved.

Keywords: Steel heat treatment; Retained austenite; Carbon partitioning; Carbide precipitation; Bainite transformation

1. Introduction

Conventional quenching and tempering heat treatments have long been applied to steels to produce good combinations of strength and toughness from the martensitic structure (e.g. [1]). More recently, austempering treatments in the bainitic region have been applied to steels alloyed with, for example, Si, which suppresses bainitic carbide formation such that carbon-enriched untransformed austenite is chemically stabilized (e.g. [2–4]). The resulting microstructure of bainitic ferrite laths, intertwined with interlath retained austenite films, rather than the ferrite/carbide combinations usual for pearlitic, bainitic or tempered martensitic structures, has promoted the potential for attractive properties in, for example, formable sheet steels (e.g. [5,6]) and high strength experimental steels [7–12], as well as austempered ductile irons (e.g. [13–18]). The present paper describes a third way: a new heat treatment that produces a microstructure that also comprises an aggregate of ferrite and carbon-enriched stabilized austenite, from austenite partially quenched to martensite rather than transformed to 'carbide-free bainite' [19–22]. Using martensite, rather than bainitic ferrite, has the immediate attraction of attaining potentially higher strength levels. The heat treatment sequence involves quenching to a temperature between the martensite-start (M_s) and martensite-finish (M_f) temperatures, followed by a 'partitioning' treatment either at, or above, the initial quench temperature, designed to enrich the remaining untransformed austenite with carbon, escaping from the supersaturated martensite phase, thereby stabilizing retained austenite phase to room temperature. Carbon partitioning between martensite and retained austenite has been discussed in early literature (e.g. [23]), but as far as the authors are aware, the concept of using carbon partitioning from martensite to stabilize retained austenite has never been developed towards a steel heat treatment process. As for the case of bainitic structures, suitable alloying must be used to suppress competing reactions, which in this instance could include decomposition to bainite and pearlite, as well as carbide precipitation. This procedure
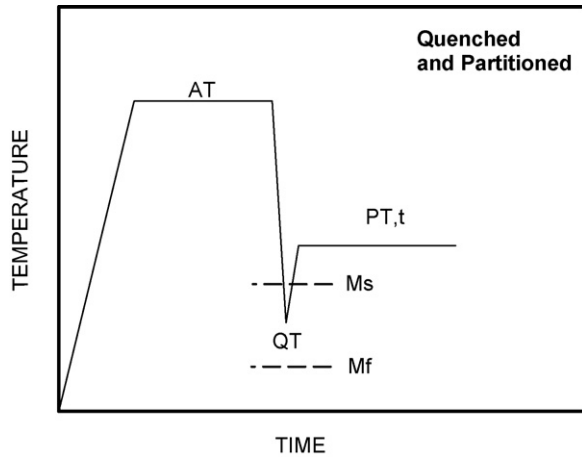

Fig. 1. Schematic Q&P heat treatment: austenitizing at AT is followed by quenching to transform partially to martensite at QT, before partitioning carbon at PT. (Compare with a bainitic austempering treatment, which would quench directly to PT, or conventional martensite Q&T, where the quench temperature would be preferably $<M_f$.)

(Fig. 1) has been termed 'quenching and partitioning' (Q&P), to distinguish it from quenching and tempering (Q&T).

2. Background and quench and partitioning fundamentals

2.1. Carbon partitioning: thermodynamics and kinetics

Although the existence of carbon-enriched retained austenite in martensitic steel microstructures has been known for some time [23–25], the process of partitioning from the supersaturated martensite to the untransformed austenite has received little attention because the essential elimination of carbon supersaturation in the martensite is ordinarily accomplished by carbide precipitation during tempering [26]. To stabilize the microstructure the decomposition of any retained austenite phase in tempered martensitic steels is also generally necessary, contrary to the present approach, and is also achieved by tempering. Thus, it was first necessary to construct a model addressing carbon partitioning from as-quenched martensite into untransformed

austenite [19]. This model assumed conditions where competing reactions are suppressed to predict the endpoint of partitioning, when the martensitic ferrite is in metastable equilibrium with austenite. This model also demonstrated the potential of this new heat treatment approach.

Metastable equilibrium between austenite and ferrite under conditions where long-range diffusion of carbon occurs but partitioning of slow-moving substitutional elements is difficult, is described by paraequilibrium [27–29], although this concept is normally applied during transformation and thus when interface migration is occurring. Thus, the ferrite/austenite phase fractions can adjust to ensure that the requirement for equal chemical potentials of each component (Fe, substitutionals and C) in both ferrite and austenite is met. In the present case the interface between martensite and untransformed austenite is assumed to be stationary. The metastable ferrite/austenite equilibrium reached by the completion of carbon partitioning in this case of an immobile or constrained interface between the two phases has thus been termed "constrained carbon equilibrium" or CCE [19,30–33]. This situation is described by two conditions: equal chemical potential of carbon in each phase, and conservation of iron (and substitutional) atoms in each phase. Fig. 2(b) illustrates the thermodynamic condition of CCE for two arbitrary examples, where the tangents to the ferrite and austenite Gibbs energy curves intersect the carbon axis at a single point, indicating equal carbon potentials in ferrite and austenite, but where the chemical potential of iron is clearly different in each phase. It can be seen that an infinite set of possible ferrite and austenite phase compositions exists, but the conservation condition of the matter balance uniquely determines the applicable phase compositions. For CCE the phase fractions are determined by the extent of the martensite reaction at the quench temperature and not by the lever rule applied using an equilibrium or paraequilibrium tie-line. Thus, by combining the thermodynamic requirement with the mass balance requirement (due to the phase fractions fixed by the quench and consequential constraint of the interface), it has been possible to calculate the extent of carbon partitioning and hence austenite stabilization, according to the total carbon concentration and volume fractions of martensite and untransformed austenite determined by the quench temperature (obtainable from the Koistinen and Mar-
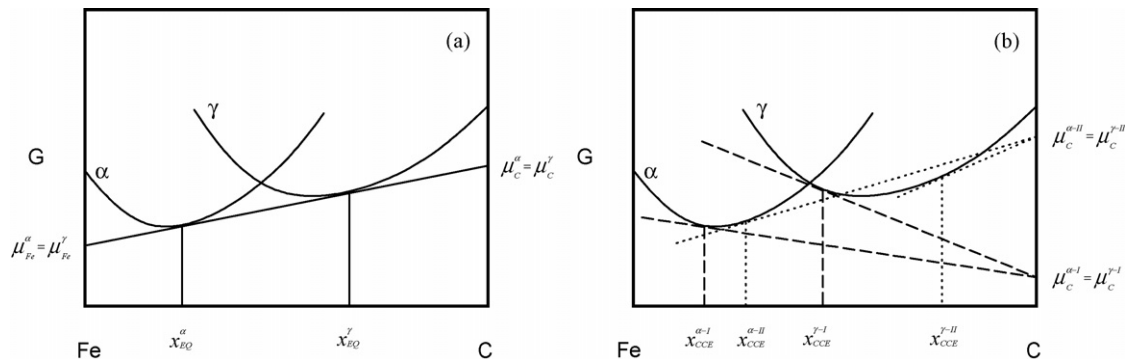

Fig. 2. Schematic molar Gibbs energy vs. composition diagrams illustrating metastable equilibrium at a particular temperature between ferrite and austenite in the Fe–C binary system: (a) equilibrium and (b) two possible constrained carbon equilibrium conditions (I and II) showing two possible ferrite and austenite compositions satisfying the CCE requirement that the chemical potential of carbon is equal in the two phases [19].
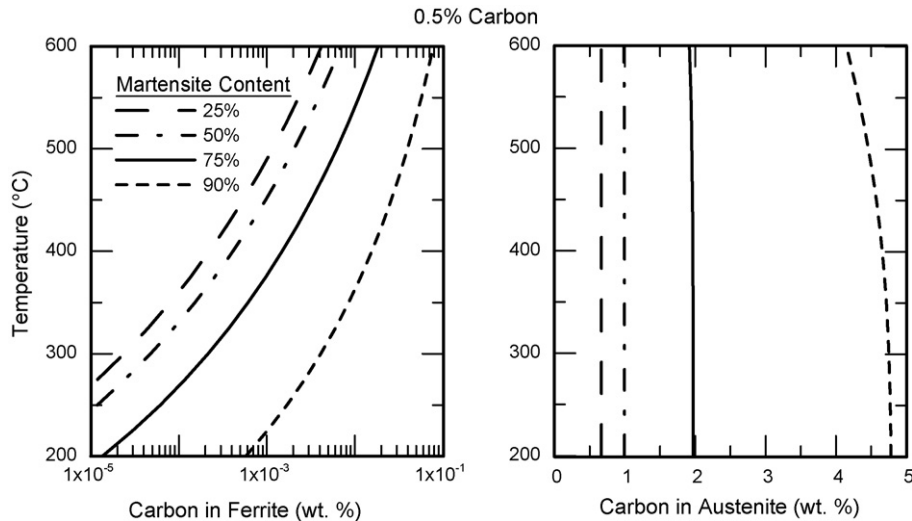
Fig. 3. Constrained carbon equilibrium calculations for Fe–0.50% C (wt.%) showing carbon concentrations in ferrite and austenite as a function of partitioning temperature for different martensitic ferrite and austenite volume fractions (determined by the quench temperature) (molar basis) [19].

burger relationship) [19,34]. This has shown that most of the carbon in the steel is expected to partition to the austenite, and thus quite high levels of carbon enrichment (Fig. 3), and hence strong austenite stabilization, are possible.

Fig. 3 also demonstrates how a very high carbon concentration could be achieved by quenching to a low temperature between M_s and M_f, giving a relatively small volume fraction of untransformed austenite to receive the carbon supersaturation, from the balancing high volume fraction of martensite, during the subsequent partitioning treatment. In this respect, Q&P could well be differentiated from the formation of the ferrite/retained austenite microstructure via transformation to carbide-free bainite, because in the latter case there is likely to be some linkage between carbon partitioning and bainitic ferrite formation, whereas in Q&P the two can be decoupled. Thus, the Q&P procedure, giving greater control over the respective volume fractions of martensitic ferrite and untransformed austenite, can make possible potentially very high carbon concentrations in the austenite.

The escape of carbon from the martensite to the untransformed austenite during the partitioning treatment is a critical step for the Q&P process, since it competes with the formation of carbides in the martensite, the normal characteristic of the tempering process. In order to estimate the time necessary for the depletion of carbon from martensite, and its homogenization in the adjacent austenite, a series of simulations was performed, using the software DICTRA [35]. The calculation models the one-dimensional escape of carbon normal to the planar interface of a martensitic ferrite lath or plate into the adjacent austenite, assumed also to be plate shaped, and with identical composition, using the assumption that only carbon equilibrates its chemical potential at the interface [36]. For a steel with composition 0.19% C–1.59% Mn–1.63% Si (wt.%), and a simulation of partitioning at 400 °C, for average thicknesses of 0.3 and 0.14 μm for the ferrite and austenite plates, respectively, based upon microstructural observation by transmission electron microscopy, Fig. 4(a) shows the variation of

the carbon concentration profile in the ferrite for times ranging from 0.0001 to 10 s, whilst Fig. 4(b) shows the corresponding profiles in the austenite. Each figure relates to a half plate, with the centre at the left and the interface to the right. The calculations show, for this particular combination of steel composition, partitioning temperature and microstructure, that the martensitic ferrite plate is depleted in less than 1 s, whilst it takes around 10 s to homogenize the austenite. The escape path of the carbon between the martensitic plate and the austenite may be different to that assumed because the exact morphology and distribution of the untransformed austenite regions within the partially transformed microstructure are not known precisely, and might be expected to differ, for example, with steel composition (martensite type) and whether the untransformed austenite is interlath films (as supposed here) or interpacket pools. Early studies of quenched martensites recorded different austenite lattice parameters in the same specimen thought to be due to separate carbon concentrations [37]. However, the calculations indicate that the carbon is likely to partition in times well within those customarily used for some industrial heat treatments.

2.2. Design of heat treatment

A schematic diagram summarizing the sequence of microstructural evolution from homogeneous austenite during Q&P processing is presented in Fig. 5 [20,21]. Following austenitization the steel is quenched to a temperature (QT) calculated to produce a pre-determined fraction of martensite and balancing fraction of untransformed austenite. The steel is then raised to the partitioning temperature (PT), when carbon escapes into the untransformed austenite, raising its chemical stability so that after subsequent cooling to ambient after partitioning, austenite is retained. As the untransformed austenite is enriched with carbon during partitioning, its effective M_s–M_f temperature range is suppressed. For complete chemical stabilization the M_s must be depressed to room temperature or below, thus, also included in Fig. 5 is the possibility to produce some additional (as-quenched)
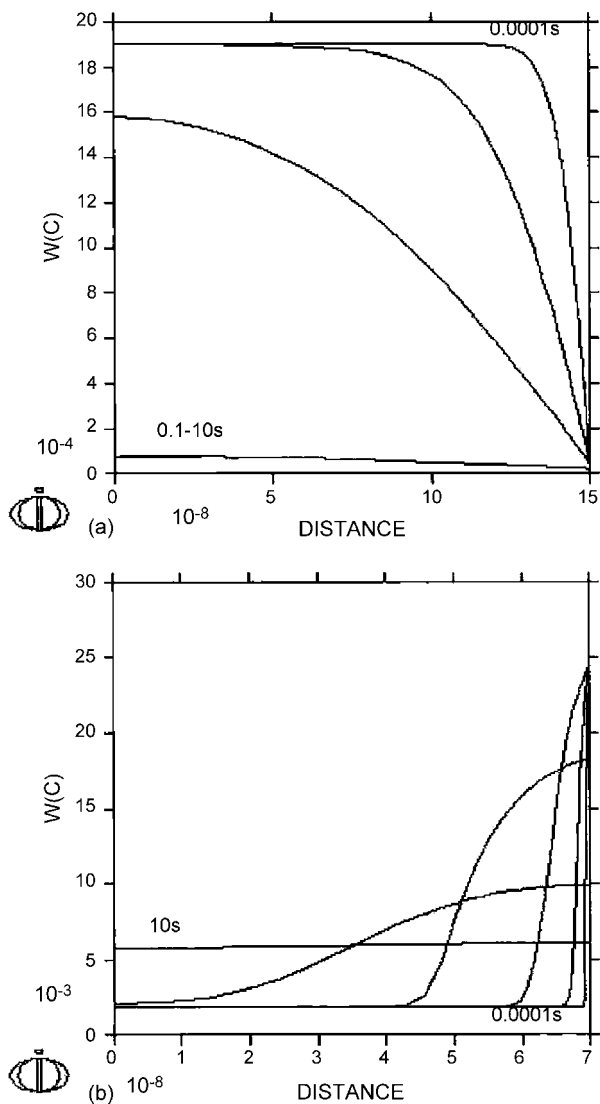
Fig. 4. Calculation of the carbon concentration profiles in wt.% ($\times 10^{-4}$) normal to the planar interface for (a) a martensite plate and (b) an adjacent austenite plate-shaped region, for times of 0.0001, 0.001, 0.01, 0.1, 1 and 10 s, in Fe–0.19% C–1.59% Mn–1.63% Si (wt.%) partitioned at 400 °C. (Both figures represent a half-plate width in metres ($\times 10^{-8}$), with centre on the left and interface on the right.) The curves for the three longer times in (a) overlap because the martensite plate is depleted of carbon within 1 s.

martensite from insufficiently stabilized austenite during this final quenching stage. This martensite will be different to that previously formed as it will normally be expected to inherit a higher carbon concentration. In addition, as discussed below, bainite might also result from transformation of untransformed austenite at longer partitioning times, and might be 'carbide-free' due to the effect of the alloying elements.

The different heat treatment schedule for processing TRIP sheet steel by Q&P would lead to modified behaviour. In this case, an intercritical solution treatment is carried out in the two-phase region so that the starting microstructure is a mixture of austenite and ferrite. It is to be noted that in this case the overall carbon concentration of the steel will be largely concentrated into the smaller volume fraction of austenite before quenching. As for conventional TRIP steel processing, the potential for sta-

bilizing the austenite is therefore enhanced (lower M_s) compared with heat-treating homogeneous austenite.

A simple method for determining the optimum quench temperature to maximize austenite stabilization and retention after full Q&P treatment has been developed [20]. This model assumes that competing reactions are avoided and that all of the carbon partitions from martensite to austenite. First, the relative fractions of martensite and untransformed austenite at the quench temperature are calculated from the undercooling below M_s, based upon the Koistinen–Marburger relationship [20,34], with the M_s for the applicable austenite carbon content estimated from published correlations. In the case of an intercritical anneal for producing a TRIP steel microstructure, it can be assumed that all of the carbon is in the austenite prior to quenching, as the solubility of ferrite for carbon is very low. Then, by applying the
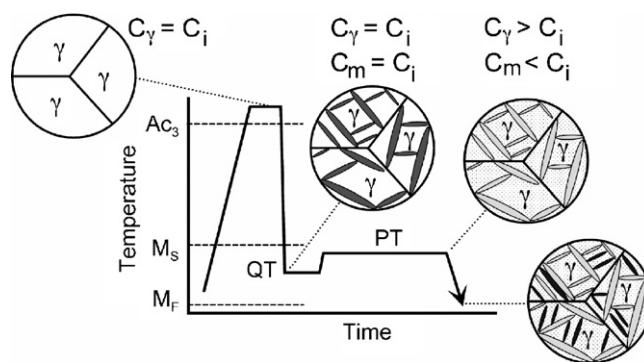

Fig. 5. Schematic diagrams of the Q&P process, producing ferrite/austenite/martensite microstructures, as appropriate, from homogeneous austenite [20,21]. (C_i, C_γ and C_m represent the carbon contents of the initial alloy, austenite and martensite, respectively, and QT and PT are the quenching and partitioning temperatures, respectively.)
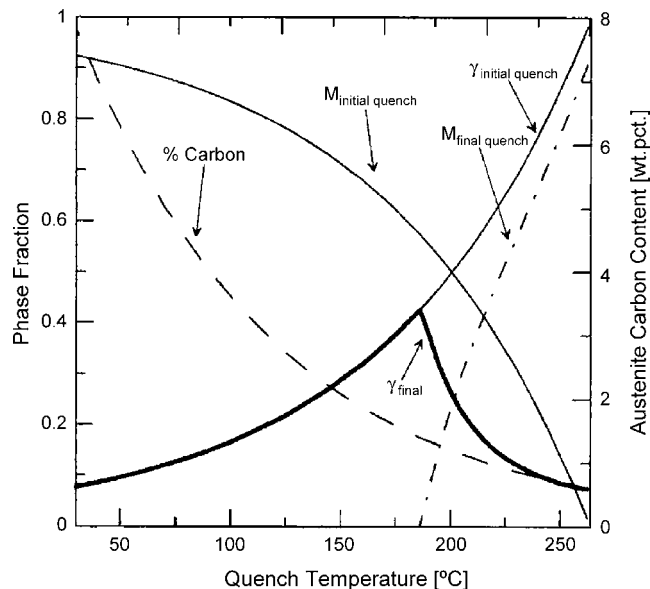

Fig. 6. Predicted components of the microstructure after Q&P treatment for an experimental steel [38]. The solid bold line gives the final austenite fraction at room temperature. Other lines represent the austenite (γ) and martensite (M) present at the initial quench temperature, and the additional martensite formed during the final quench to room temperature.

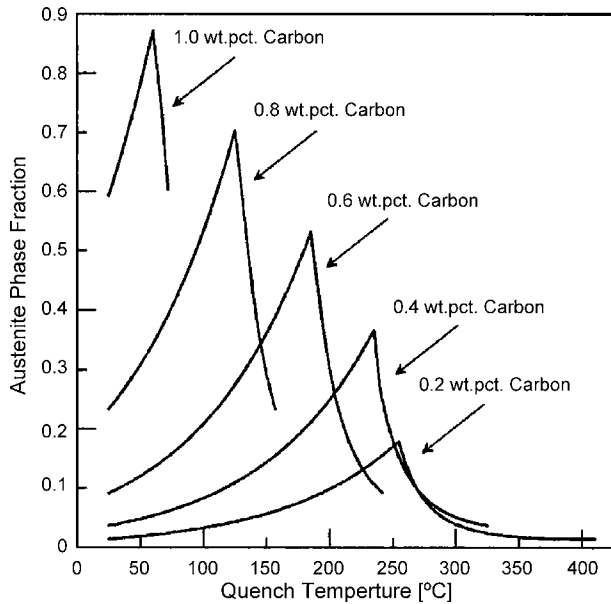Fig. 7. Predicted amount of retained austenite for different carbon contents [38].
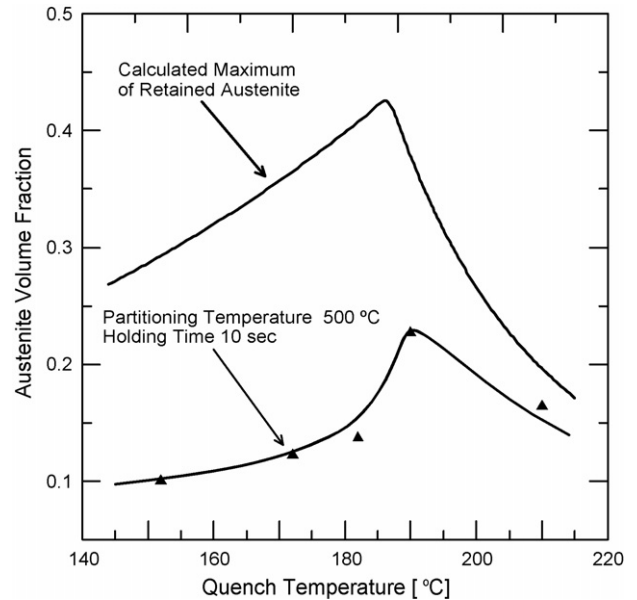

Fig. 8. Final volume fraction of retained austenite measured after partitioning 10 s at 500 °C, as a function of quench temperature, and the calculated maximum fraction achievable by full partitioning over this quench temperature range [38].

Koistinen–Marburger relationship again, this time to the carbon-enriched untransformed austenite fraction after full partitioning, the final phase fractions after final cooling can be predicted.

Fig. 6 illustrates the predicted evolution of microstructure according to this methodology [20,38]. This indicates an optimum quench temperature for yielding the maximum amount of retained austenite. At quench temperatures above this optimum quench temperature, substantial untransformed austenite remains after the initial quench but the carbon escaping from the lower volume of martensite is insufficient to stabilize austenite such that fresh martensite is formed during quenching to room temperature. Below the optimum quench temperature too much austenite is transformed by the initial quench (although sufficient partitioned carbon is available for its complete stabilization). The optimum quench temperature is where just the right amount of martensite is formed during the initial quench to enrich the untransformed austenite after full partitioning to reduce its M_s temperature to room temperature.

Fig. 7 illustrates how this model predicts the increase in final austenite fraction as a function of the initial carbon content of the steel [38]. The figure was originally constructed to consider the response of a carburized component during Q&P processing, and illustrates the importance of carbon in stabilizing austenite and influencing relevant processing temperatures.

3. Experimental observations and applications

A number of experimental and commercial steel compositions that have so far been examined are given in Table 1. These have been mainly representative of medium carbon bar steels and lower carbon sheet steels, with enhanced Si or Al addition. The Q&P heat treatments comprised: for medium carbon levels—austenitizing at 900 °C for 300 s followed by
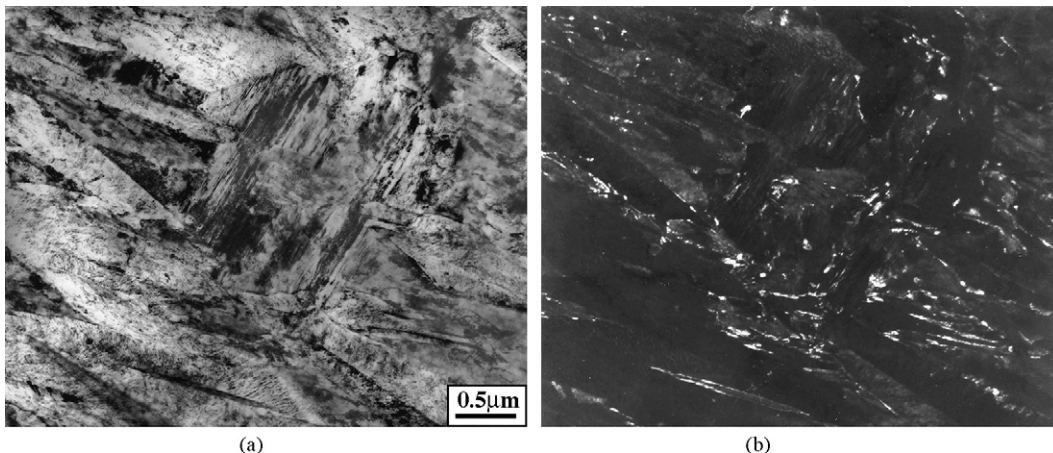

Fig. 9. Electron micrographs of grade 9260 steel quenched to 190 °C, held for 120 s, and then quenched to room temperature: (a) bright-field image and (b) dark-field image using (0 0 2) austenite reflection [22].

quenching to the range 150–210 °C and partitioning in the range 250–500 °C for 10–3600 s; for low carbon levels—annealing at various temperatures for 180 s followed by quenching to 220 °C and partitioning in the range 350–450 °C for 3 s. Salt baths were used for austenitizing and partitioning treatments,

and a tin–bismuth bath for the lower quench temperatures; final quenching was into water. The microstructural changes developed during the Q&P treatment were basically similar across this range of steels, and so are highlighted and discussed here mainly for the 0.6 wt.% C bar steel.
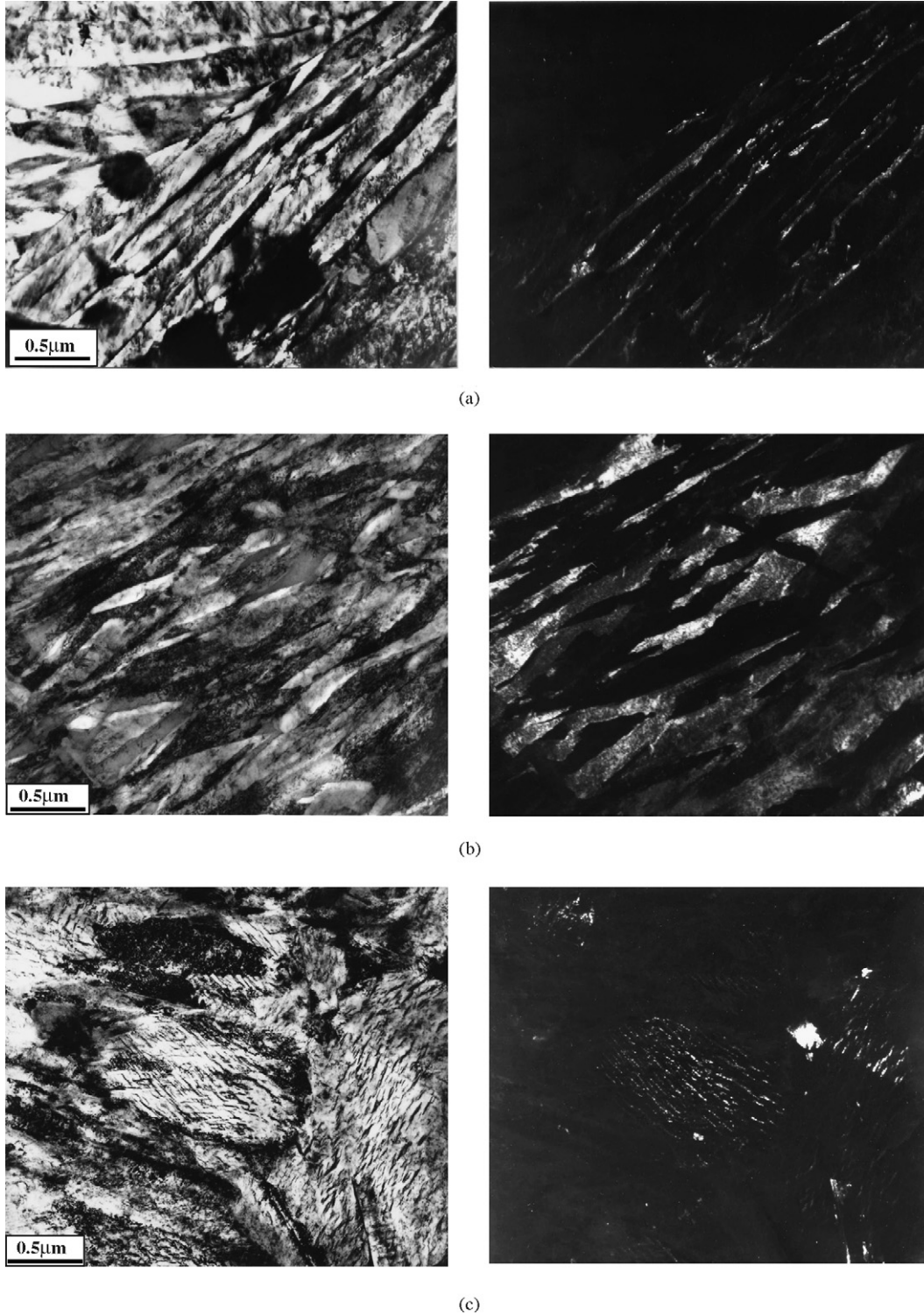

(a)

(b)

(c)

Fig. 10. Electron micrographs of grade 9260 steel: (a) quenched 190 °C and partitioned at 250 °C (bright field and dark field using (0 0 2) austenite reflection), (b) quenched 190 °C and partitioned at 400 °C (bright field and dark field using (0 0 2) austenite reflection) and (c) quenched 150 °C and partitioned at 250 °C (bright field and dark field using (1 $\bar{1}$ 1) epsilon carbide reflection).

Fig. 8 shows the variation in retained austenite fraction, measured by X-ray diffraction analysis, after Q&P treatment in bar steel grade 9260 (Fe–0.60% C–0.95% Mn–1.96% Si (wt.%)) as compared with the maximum austenite achievable according to the model described above (Fig. 6) [38]. It can be seen that the austenite phase fraction follows the predicted relationship with quench temperature for this partitioning treatment, but at a reduced level. This indicates the probable intervention of competing reactions that has lowered the concentration of carbon escaping to the untransformed austenite during the partitioning treatment.

3.1. Microstructures and competing reactions

Fig. 9 shows a typical martensitic microstructure, produced by an initial quench to the quench temperature, equilibration for 120 s, followed by a final quench to room temperature [22]. More retained austenite (>6%) was obtained by this treatment compared with that obtained by direct quenching to room temperature (<2%), indicative of some carbon partitioning from the martensite during the holding time at the quench temperature [38]. However, even after 120 s at this quench temperature of 190 °C there is some evidence for carbide precipitation in the martensitic ferrite in the bright-field micrograph (Fig. 9(a)). Apart from highlighting the competition for carbon, this is also plausible confirmation that this martensite had formed at the quench temperature. It also reveals that carbide could already be present in the martensite before it is raised to the partitioning temperature. If this is transitional carbide, which is most likely, having formed at low temperature, then it could conceivably re-dissolve at the higher partitioning temperature, providing a source of carbon, either for equilibrium cementite formation, or for further enrichment of untransformed austenite.

Detailed observations by high-resolution electron microscopy have been made over a range of quench and partitioning temperatures and a selection of microstructures is presented in the electron micrographs of Fig. 10. Fig. 10(a) shows thin films of retained austenite between martensite laths after partitioning at 250 °C, and can be compared with Fig. 10(b) showing the thicker retained austenite films observed after partitioning at a higher temperature of 400 °C. The main reason for the reduced austenite retention at the lower partitioning temperatures is due to competition with carbide precipitation. Fig. 10(c) shows copious carbide precipitation typical of that observed over the lower range of partitioning temperatures. This carbide was identified as the transitional epsilon carbide. It would thus appear that the alloying elements deployed to

Table 1
Concentration (wt.%) of principal elements in experimental steels

	C	Mn	Si	Al
Bar	0.60	0.95	1.96	–
Sheet	0.35	1.30	0.74	–
	0.19	1.59	1.63	–
	0.19	1.46	0.02	1.96

inhibit carbide reactions were ineffective in suppressing the occurrence of this phase. The dominant carbide at higher partitioning temperatures was cementite, for which the alloying did appear to be effective in suppressing its precipitation, such that for shorter times at the partitioning temperature very little cementite was detected, thereby giving ample time for enrichment of the untransformed austenite.

It has been known for a long time that silicon influences the sequence of reactions customarily observed during the tempering of martensitic steels (e.g. [39,40]). It exerts similar effects upon the course of the bainite reaction (e.g. [2–4,37,41]). In particular, it retards the formation of cementite—this can delay the progress of Stage 3 tempering of martensite (principally, the formation of cementite at the expense of transitional epsilon carbide) or the formation of cementite during the bainite transformation, resulting in 'carbide-free' bainite. At the same time, silicon appears to stabilize the transitional epsilon carbide, which consequently persists for longer times and to higher temperatures. Its suppression of cementite is usually explained by its low solubility in cementite, and thus a need to diffuse away from the growing carbide [39], and there is experimental evidence that Si is indeed rejected into the surrounding ferrite [42]. In contrast, the stabilization of epsilon carbide was thought to be due to higher silicon solubility in this transitional carbide [40], but measurements by microanalytical transmission electron microscopy and atom-probe techniques have not indicated a particularly high level of enrichment [42]. Aluminium is thought to behave similarly to silicon in retarding tempering reactions, but there has been less study of its detailed effect upon the carbide reactions [43].

This respective carbide precipitation may be interpreted to conform with the schematic C-curve behaviour depicted by Fig. 11, which suggests separate C-curves over different temperature ranges for the transitional carbide and cementite, respectively [44,45]. Fig. 11 also illustrates cementite precipitation delayed by alloying to present a temperature/time window for the partitioning heat treatment. The lowest partitioning temperature to achieve effective maximum austenite stabilization in the steels examined is thus defined by the appearance of the transitional epsilon carbide.

The behaviour in one steel recorded so far can thus be summarized by Fig. 12, constructed from experimental data obtained over a range of quench and partitioning temperatures [38]. This demonstrates how the effect of transitional carbide precipitation in the lower partitioning temperature range dramatically reduces the maximum retained austenite achievable by Q&P treatment. This diagram indicates how Fig. 8 (showing data for one partitioning temperature) changes over a range of partitioning temperatures. It is clear that in order to expand the Q&P heat treatment window to lower partitioning temperatures, which may be desirable for application to some industrial processes, the transitional carbide reaction within the martensitic ferrite must be suppressed. Some consolation can be gained, however, from the results of the kinetic modelling, which shows that precipitation need not be delayed for too long in order to give time for the majority of carbon to escape the martensitic laths.
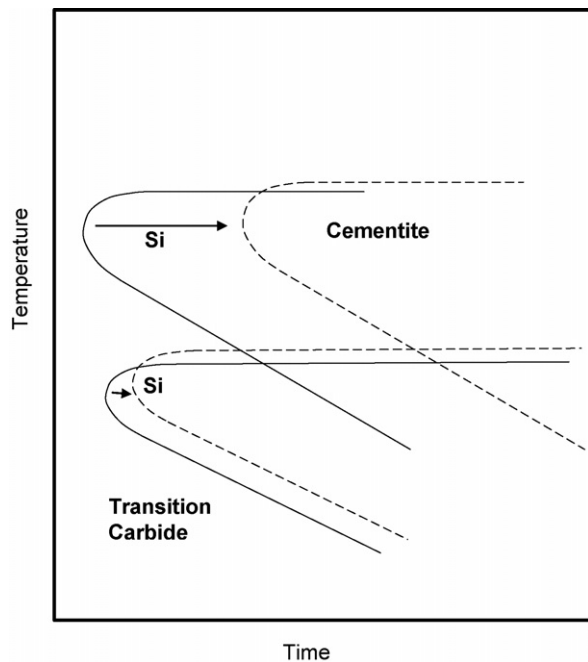
Fig. 11. Schematic C-curves indicating the effect of Si alloying on carbide precipitation kinetics.

Another reaction within the martensitic ferrite could be carbon trapping at the defect structure. Substantial carbon trapping at dislocations could in some cases influence the levels available for stabilization of austenite. It is difficult to draw any inferences about carbon atom trapping from the electron microscope observations, except that the dislocation substructure in the martensitic ferrite was much reduced at the higher partitioning temperatures, for example, Fig. 10(b) as compared with Fig. 10(a), which might imply less restraint on dislocation mobility by carbon during recovery, but clearly this could solely be a thermal effect, as would be expected. The observation of reduced substructure, however, could inform predictions of final mechanical behaviour.

Alternative reactions affecting carbon enrichment and retention of the untransformed austenite could be decomposition of
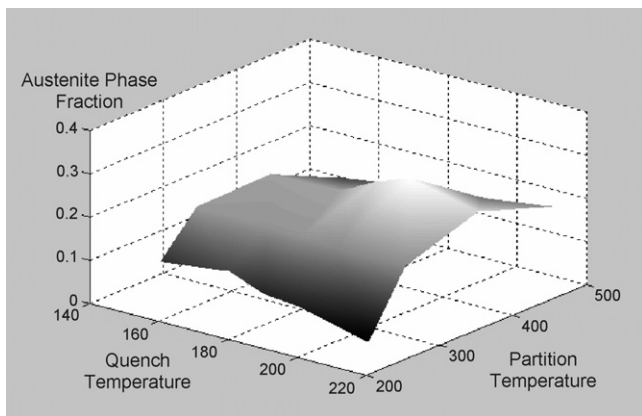

Fig. 12. Variation of retained austenite fraction as a function of both quench temperature and partitioning temperature, for short partitioning times <120 s, after [38].
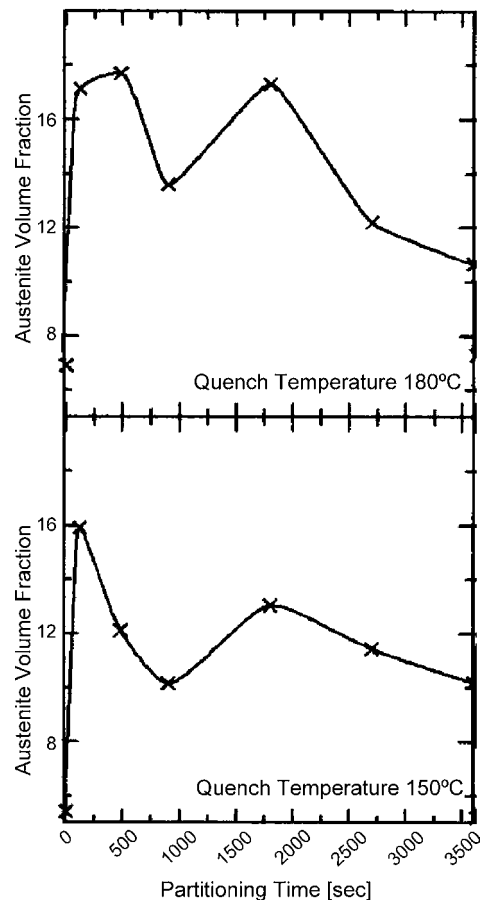

Fig. 13. Variation of retained austenite fraction as a function of partitioning time, after [38].

untransformed austenite during the partitioning treatment to carbides, bainite or even pearlite at sufficiently high partitioning temperatures. Fig. 13 shows the effect of partitioning time on the final level of retained austenite [38]. A rapid stabilization of austenite is indicated at very short times, consistent with the rapid kinetics of escape of carbon from the martensite into the untransformed austenite. Interestingly, however, these preliminary data also revealed the possibility for a second peak of retained austenite before the level generally falls off with increasing partitioning time. The error in quantification of the austenite fraction is stated as 2% and so this behaviour needs further investigation, but one explanation for the appearance of a second peak at intermediate partitioning times, if indeed a real effect, might be re-solution of transitional carbides formed at lower temperatures (Fig. 9). It is assumed that the kinetics of this reaction would be slower than that of the initial rapid partitioning of carbon to the untransformed austenite (Fig. 4). As the formation of cementite would be suppressed by the alloying, the carbon released from the transitional carbide would be available for a second wave of carbon enrichment, or carbon replenishment (as the austenite is already less stabilized) leading to a second peak of austenite stabilization, as observed.

After an initial short period of carbon partitioning, the overall long-term trend is for a reduction in retained austenite with partitioning time, which can be explained by carbide precipitation,

probably occurring at the austenite/martensitic ferrite interfaces. This would be equivalent to the usual explanation for the formation of interlath carbide in bainite. It is reported [46] that carbide precipitation from untransformed interlath austenite observed in the lower bainite reaction is much slower than the dominant carbide precipitation that occurs within the bainitic ferrite.

4. Summary

The potential to produce useful ferrite/retained austenite microstructures by means of a novel heat treatment route, termed quenching and partitioning, which utilizes the martensite transformation, has been described. Substantial volumes of stabilized austenite have been achieved, using heat treatments based upon a model assuming full carbon partitioning, verifying that the proposed Q&P treatment can succeed. Steel compositions so far examined have been based upon medium carbon bar steels, e.g. grade 9260, and formable TRIP-aided sheet steels.

By considering thermodynamic and kinetic models for the evolution of the microstructure, and studying the microstructures produced by high-resolution electron microscopy, it is shown or suggested that the Q&P process has the potential for the control of a variety of microstructural conditions, including:

(i) The ratio of martensitic ferrite and retained austenite volume fractions, by choice of quench temperature.
(ii) The nature of the martensite produced, lath or twin, thereby influencing the form of the 'partitioned' martensitic ferrite, by altering steel carbon content, or austenite carbon concentration by intercritical annealing treatments.
(iii) Possible variation of the dislocation substructure and carbon concentration in the martensitic ferrite, by control of partitioning treatment, to influence strength.
(iv) Variation of carbon concentration and hence stabilization and properties of untransformed/retained austenite, by control of partitioning treatment. (The level of carbon enrichment of untransformed austenite is potentially very high if competing reactions are totally suppressed and the overall carbon concentration of the steel partitioned to a relatively small volume fraction of untransformed austenite.)
(v) Development of a mixed martensitic ferrite/bainitic ferrite/retained austenite microstructure by allowing some decomposition to carbide-free bainite at longer partitioning times.
(vi) The generation, if required, of a dispersion of 'fresh' as-quenched martensite laths in the microstructure, by control of carbon enrichment of the untransformed austenite such as to allow some decomposition on cooling to room temperature.

The microstructure of ferrite laths separated by films of retained austenite is somewhat similar to (though usually somewhat finer than) that produced by bainitic reaction in steels similarly alloyed to suppress carbide formation. However, a main advantage of proceeding by this novel heat treatment route would be the potential for greater control over evolution of the microstructure, especially the level to which the untransformed

austenite could be enriched, which initially is decoupled from the austenite–ferrite phase transformation. However, the partitioning treatment could also involve bainite transformation at longer times, possibly required by some industrial processes, but because a similar microstructure would result, this would not be expected to diminish greatly, if at all, the mechanical properties.

Further work, both fundamental and applied, is required to examine the competing reactions, especially alloying effects on carbide formation, and the kinetics of the reactions, and to test and optimize alloy/microstructure/property combinations and incorporate mill processing considerations, in order to clarify the potential benefits of this innovative martensite heat treatment procedure.

References

[1] G. Krauss, P.E. Repas (Eds.), Fundamentals of Aging and Tempering in Bainitic and Martensitic Steel Products, ISS-AIME, Warrendale, PA, USA, 1992.
[2] R.F. Hehemann, Phase Transformations, ASM, Metals Park, OH, USA, 1970, pp. 397–432.
[3] H.K.D.H. Bhadeshia, D.V. Edmonds, Metall. Trans. 10A (1979) 895–907.
[4] H.K.D.H. Bhadeshia, Bainite in Steels, Institute of Materials, Minerals and Mining, London, UK, 1992.
[5] B.C. De Cooman (Ed.), TRIP-Aided High Strength Ferrous Alloys, International Conference Proceedings, Technologisch Instituut VZW, 2002.
[6] J.G. Speer (Ed.), Advanced High-Strength Sheet Steels for Automotive Applications, International Conference Proceedings, AIST, Warrendale, PA, USA, 2004.
[7] H.K.D.H. Bhadeshia, D.V. Edmonds, Met. Sci. J. 17 (1983) 411–419.
[8] H.K.D.H. Bhadeshia, D.V. Edmonds, Met. Sci. J. 17 (1983) 420–425.
[9] V.T.T. Miihkinen, D.V. Edmonds, Mater. Sci. Technol. 3 (1987) 422–431.
[10] V.T.T. Miihkinen, D.V. Edmonds, Mater. Sci. Technol. 3 (1987) 432–440.
[11] V.T.T. Miihkinen, D.V. Edmonds, Mater. Sci. Technol. 3 (1987) 441–449.
[12] F.G. Caballero, H.K.D.H. Bhadeshia, K.J.A. Mawella, D.G. Jones, P. Brown, Mater. Sci. Technol. 17 (2001) 512–522.
[13] W.J. Dubensky, K.B. Rundman, AFS Trans. 64 (1985) 389–394.
[14] V. Franetovic, M.M. Shea, E.F. Ryntz, Mater. Sci. Eng. 96 (1987) 231–245.
[15] N. Darwish, R. Elliott, Mater. Sci. Technol. 9 (1993) 572–602.
[16] L. Sidjanin, R.E. Smallman, S.M. Boutorabi, Mater. Sci. 10 (1994) 711–720.
[17] J. Aranzabel, I. Gutierrez, J.J. Urcola, Mater. Sci. Technol. 10 (1994) 728–737.

[18] A. Honarbakhsh-Raouf, D.V. Edmonds, Electron Microscopy, ICEM 14, vol. II, Mater. Sci. (1998) 173–174.

[19] J.G. Speer, D.K. Matlock, B.C. De Cooman, J.G. Schroth, Acta Mater. 51 (2003) 2611–2622.

[20] J.G. Speer, A.M. Streicher, D.K. Matlock, F.C. Rizzo, G. Krauss, in: E.B. Damm, M. Merwin (Eds.), Austenite Formation and Decomposition, TMS/ISS, Warrendale, PA, USA, 2003, pp. 505–522.

[21] D.K. Matlock, V.E. Brautigam, J.G. Speer, THERMEC'2003, Trans Tech Publications, Uetikon-Zurich, Switzerland, 2003, pp. 1089–1094.

[22] J.G. Speer, F.C. Rizzo, D.K. Matlock, D.V. Edmonds, 59th Annual Congress of ABM, Sao Paulo, 2004, pp. 4824–4836.

[23] S.J. Matas, R.F. Hehemann, Nature 187 (1960) 685–686.

[24] B.V.N. Rao, G. Thomas, International Conference on Martensitic Transformations ICOMAT'79, Mass. Inst. Technol., USA, 1979, p. 12.

[25] M. Sarikaya, G. Thomas, J.W. Steeds, S.J. Barnard, G.D.W. Smith, in: H.I. Aaronson (Ed.), Solid to Solid Phase Transformations, TMS, Warrendale, PA, USA, 1982, pp. 1421–1425.

[26] C.S. Roberts, B.L. Averbach, M. Cohen, Trans. ASM 45 (1953) 576.

[27] A. Hultgren, Trans. ASM (1947) 915.

[28] M. Hillert, Jernkont. Ann. 136 (1952) 25.

[29] E. Rudberg, Jernkont. Ann. 136 (1952) 91.

[30] M. Hillert, J. Agren, Scripta Mater. 50 (2004) 697–699.

[31] J.G. Speer, D.K. Matlock, B.C. De Cooman, J.G. Schroth, Scripta Mater. 52 (2005) 83–85.

[32] M. Hillert, J. Agren, Scripta Mater. 52 (2005) 87–88.

[33] John G. Speer, David V. Edmonds, Fernando C. Rizzo, David K. Matlock, Curr. Opin. Solid State Mater. Sci. 8 (2004) 219–237.

[34] G. Krauss, Steels: Heat Treatment and Processing Principles, ASM International, Metals Park, OH, USA, 1990.

[35] A. Borgenstam, A. Engstron, L. Hoglund, J. Agren, J. Phase Equilib. 21 (2000) 269–280.

[36] M. Hillert, L. Hoglund, J. Agren, Acta Metall. Mater. 41 (1993) 1951–1957.

[37] S.J. Matas, R.F. Hehemann, Trans. Met. Soc. AIM 221 (1961) 179–185.

[38] F.L.H. Gerdemann, Microstructure and hardness of 9260 steel heat-treated by the quenching and partitioning process, Diploma Thesis, Aachen University of Technology, Germany, 2004.

[39] W.S. Owen, Trans. ASM 46 (1954) 812–829.

[40] J. Gordine, I. Codd, J. Iron Steel Inst. 207 (1969) 461–467.

[41] B.P.J. Sandvik, Metall. Trans. A13 (1982) 777–787.

[42] S.J. Barnard, G.D.W. Smith, A.J. Garratt-Reed, J. Vander Sande, Advances in the Physical Metallurgy and Applications of Steels, Metals Society, London, UK, 1981, pp. 33–38.

[43] W.C. Leslie, G.C. Rauch, Metall. Trans. 9A (1978) 343–349.

[44] A.S. Keh, W.C. Leslie, Material Science Research, vol. 1, Plenum Publishing, NY, USA, 1963, pp. 208–250.

[45] G.M. Michal, J.A. Sloane, Metall. Trans. 17A (1986) 1287–1294.

[46] H.K.D.H. Bhadeshia, Acta Metall. 28 (1980) 1103–1114.